

THE BLACK HOLE BINARY A0620–00

JEFFREY E. MCCLINTOCK¹

Department of Physics and Center for Space Research, Massachusetts Institute of Technology; and
 Harvard-Smithsonian Center for Astrophysics

AND

RONALD A. REMILLARD¹

Center for Space Research, Massachusetts Institute of Technology

Received 1985 November 21; accepted 1986 February 7

ABSTRACT

Photometric observations of the X-ray nova A0620–00 in quiescence during 1981–1985 have provided a unique value of the orbital period of 7.75234 ± 0.00010 hr; radial velocity observations obtained in 1985 January have revealed that the velocity semiamplitude of the dwarf companion is 457 ± 8 km s⁻¹. The corresponding mass function is $f(M) = 3.18 \pm 0.16 M_{\odot}$. A firm lower limit (3σ) to the mass of the compact X-ray source is $3.20 M_{\odot}$; this result is independent of the distance to the source and insensitive to the assumed mass of the companion. The mass of the compact source exceeds the maximum allowed mass of a stable neutron star based on the stiffest equations of state that are considered realistic. In this sense we conclude that the compact object in A0620–00 is a black hole.

We are confident that the radial velocity data reflect the orbital motion of the K-dwarf companion because (1) the velocity data are well fitted (rms error ≈ 10 km s⁻¹) to a circular-orbit model using the precise photometric period; (2) the time of primary photometric minimum coincides with the time of zero velocity to within the observational uncertainties ($\Delta T = 5 \pm 7$ minutes); and (3) the absorption lines of a K dwarf are plainly evident in a grand-sum spectrum which has been Doppler-corrected to the rest frame of the secondary.

The radial velocity data and new I-band data confirm that the light curve is primarily due to the tidal distortion of the K dwarf. An approximate analysis of the light curve suggests that if the K dwarf fills its Roche lobe during quiescence, then the inclination of the orbit is less than 50° and the mass of the black hole exceeds $7.3 M_{\odot}$ (3σ). A0620–00 is the third X-ray binary for which there is firm dynamical evidence of a massive compact object. It is the first such system to be discovered with a late-type (low-mass) secondary.

Subject headings: black holes — stars: individual — X-rays: binaries

I. INTRODUCTION

For two months in the autumn of 1975, A0620–00 (Nova Mon 1917, 1975) was the brightest celestial X-ray source. The peak 1–10 keV X-ray luminosity was 1.0×10^{38} ergs s⁻¹ (Elvis *et al.* 1975) for a distance of 870 pc (Oke 1977). During outburst A0620–00 was identified with a blue star of twelfth magnitude (Boley *et al.* 1976). Fifteen months later the optical counterpart had returned to its preoutburst brightness ($V \approx 18.3$). Its quiescent spectrum was found to consist of two components: a K4 V–K7 V stellar spectrum and an emission-line component which was attributed to an accretion disk (Oke 1977; Whelan *et al.* 1977; Murdin *et al.* 1980).

X-ray novae comprise a small subclass of low-mass X-ray binaries (LMXB), which are systems composed of a late-type optical companion and a neutron star or a black hole (van Paradijs 1983; Bradt and McClintock 1983; Joss and Rappaport 1984). A total of ~ 40 LMXBs have been identified optically. In most LMXBs the intrinsic spectrum of the late-type companion is overwhelmed by the intense optical continuum produced by X-ray-heated gas. In quiescent X-ray novae the fraction of the light due to X-ray heating is negligible. Therefore, X-ray novae provide a rare opportunity to observe

the spectrum of the companion star in an LMXB and thereby to determine the distance, age, and orbital parameters of the binary system. Consequently, in 1981 we began a campaign to observe the quiescent state of A0620–00, the brightest and best-studied X-ray nova. In an earlier paper on A0620–00, we reported periodic optical variations with a full amplitude of 0.2 mag (McClintock *et al.* 1983; hereafter Paper I); we suggested that the light curve is ellipsoidal and that the orbital period is 7.8 hr. These tentative conclusions are amply confirmed by the results presented in this paper. Herein we present extensive new photometric data, a precise value for the binary period, the radial velocity curve of the K-dwarf companion, and a Doppler-corrected spectrum of the companion which reveals the presence of narrow absorption lines.

II. OBSERVATIONS

a) Photometry

Photometry data were obtained with a CCD camera, the MASCOT (Ricker *et al.* 1981, and references therein), on the McGraw-Hill 1.3 m telescope² during four observing runs (see Table 1). The 86 hours of useful data, which consist of 363 exposures of 10–15 minute duration, were obtained in gener-

¹ Visiting Astronomer at Kitt Peak National Observatory, National Optical Astronomy Observatories, which is operated by the Association of Universities for Research in Astronomy, Inc., under contract with the National Science Foundation.

² The McGraw-Hill Observatory, which is located on Kitt Peak, is operated jointly by the University of Michigan, Dartmouth College, and the Massachusetts Institute of Technology.

TABLE 1
JOURNAL OF OBSERVATIONS
A. PHOTOMETRIC OBSERVATIONS

Observing Run	UT Dates	Start Time JD 2,444,900+	Number of CCD Frames	Comments
1.....	1981 Oct 29–Nov 3	6.86	62	Paper I
2.....	1982 Dec 15–Dec 20	418.73	135	43 frames are I-band data
3.....	1983 Dec 6–Dec 16	774.78	125	
4.....	1985 Jan 12–Jan 17	1177.75	41	Simultaneous photometric and spectroscopic observations on Jan 17

B. SPECTROSCOPIC OBSERVATIONS

Object Name	UT (start) 17 Jan 1985	Exposure Time (minutes)	Air Mass (start)	Comments
G191B2B	01:41	10	1.29	Flux standard
A0620-00	02:29	16	1.99	
A0620-00	03:19	16	1.57	
A0620-00	03:37	16	1.47	
A0620-00	04:06	16	1.36	
A0620-00	04:24	16	1.30	
A0620-00	04:49	16	1.25	
A0620-00	05:07	16	1.22	
A0620-00	05:33	16	1.19	
A0620-00	05:50	16	1.18	
A0620-00	06:15	16	1.19	
HD 88230	12:22	10	1.19	K7 comparison
HR 5256	12:42	5	1.16	K3 comparison
HR 5553	12:54	5	1.10	K2 comparison
HR 5568	13:07	5	1.84	K4 comparison
HZ 44	13:21	10	1.01	Flux standard

ally good seeing ($\sim 2''$) and with good sky transparency. About one-third of these data were obtained in the presence of cirrus clouds; however, they proved useful because the CCD camera provides simultaneous observations of numerous comparison stars. Nearly all of the data were taken in the same broad, blue-visual ("BV"; 4000–6400 Å FWHM) bandpass, which has an effective wavelength of ~ 5500 Å for a star with the observed color of A0620-00 ($B-V = 1.4$). In 1982 eight hours of data were obtained in the I band ($\lambda_{\text{eff}} = 9000$ Å). A detailed description of the observations and the data analysis techniques is given in Paper I.

b) Spectroscopy

The KPNO Intensified Image Dissector Scanner (IIDS; DeVeny 1984) and the Mayall 4 m reflector were used to make spectroscopic measurements during the night of 1985 January 17 UT. Simultaneous CCD photometry was also obtained (see Table 1). The sky was moonless during all of the observations of A0620-00 and clear throughout the night. The seeing was $3''$ – $4''$ during the first hour of the night and typically $2''$ – $3''$ thereafter. A total of ten 16 minute observations of A0620-00 were made during the first 4 hr. Because of a chronic failure in a link between the telescope and instrument computers, no data were obtained during the following 6 hr interval. During the last hour the computer link was again functioning and crucial comparison spectra of four K dwarfs were obtained. A journal of the spectroscopic observations is given in Table 1.

All of the observations were obtained with a pair of $3\frac{1}{2}''$ apertures and a 4900–5600 Å bandpass which was sampled by 1024 data channels. The spectral resolution was 3.5 Å (FWHM). During the observations of A0620-00, the aper-

tures were switched between object and sky at 4 minute intervals. Comparison lamp spectra were taken at approximately half-hour intervals, before and after each pair of observations of the object. A neutral-density filter that provided an attenuation of 10^5 was required for observations of the four bright comparison stars (see Table 1).

The data were wavelength calibrated and flux calibrated at KPNO using the Interactive Picture Processing System (IPPS) data analysis system (Barnes *et al.* 1983). In order to reduce the level of statistical noise, all of the spectra were smoothed with a three-channel running average (unweighted) which degraded the spectral resolution slightly from 3.5 to 4.0 Å (FWHM). The IPPS system was used to monitor the wavelength stability of the IIDS spectrometer by measuring the channel locations of several lines in the spectra of the comparison lamp and the night sky. In the typically half-hour intervals between lamp exposures, shifts in the locations of the calibration lines were found to be 0.1 channels or less. During the 4 hr observation of A0620-00, the wavelength calibration varied by only 0.4 channels. Moreover, these small shifts were corrected for during the analysis of the data. A further check on the stability of the final wavelength calibration was made by measuring the wavelength of the $\lambda 5574.4$ night-sky line in 32 spectra, including all 20 (object and sky) spectra of A0620-00; in each case the measured wavelength was within 0.2 Å of the expected value. Based on our findings and the experiences of other observers who have used the IIDS to measure stellar radial velocities (Goad 1985), we conclude that velocity errors due to instrumental effects are unlikely to exceed 10 km s^{-1} . A tape copy of the data in FITS format was prepared by J. Barnes, and the subsequent data analysis described below was done at our home institutions.

III. LIGHT CURVES

a) *Orbital Period*

An inspection of all of the BV-band photometric data revealed that between each observing run small secular changes (≈ 0.1 mag) occurred in the mean brightness of A0620-00 relative to the nearby comparison stars. Consequently, before combining the four data sets (see Table 1), which span a 3.2 yr interval, we normalized them to have the same intensity at primary minimum. The normalizing factors we used are 1.00, 0.91, 0.98, and 1.14, respectively; a smaller number implies the object was fainter. We then searched for periodicities by making a χ^2 fit to the entire BV-band data set using a sine-cosine series in ω , 2ω , 3ω , etc., for a wide range of trial periods (see Paper I). A fit which included only the fundamental term confirmed our earlier discovery that the system has a fundamental period near 3.9 hr (Paper I). The minimum reduced χ^2 for this fit is rather poor (3.1), in part because this model makes no distinction between the primary and secondary minima which are very different (see below). A better fit was obtained to a series with terms up to and including 5ω ($\chi^2 = 2.5$). The measurement errors and the values of χ^2 are determined from the variances of comparison stars which are comparable in brightness to A0620-00.

The 11 term fit yielded a unique value of the orbital period, 7.75234 ± 0.00010 hr; the heliocentric epoch of the primary minimum is JD 2,445,477.827 $\pm 0^d.005$. The spectroscopic data

presented below confirm that 7.75 hr, and not 3.9 hr, is the true orbital period of the system. In passing, we note that if the four data sets are not normalized to a common value at primary minimum, then the value of χ^2 is significantly larger; however, the determination of the period is not affected.

We searched for a possible change in the binary period by making independent determinations of the period for the 1981-1982 data and for the 1983-1985 data (see Table 1). The values agree with each other to within 0.1σ . The corresponding limit on the rate of change of the orbital period during the two-year interval from the middle of 1982 to the middle of 1984 is $\dot{P}/P < 2.5 \times 10^{-5} \text{ yr}^{-1}$ (1σ).

b) *Folded Data*

All of the BV data (1981-1985) were folded modulo the orbital period. The resultant light curve is shown in Figure 1a. There are two distinct minima and two maxima per orbital cycle; the time of primary minimum is defined to be photometric phase zero. The extreme range of variability from primary minimum to primary maximum is 0.22 mag. The secondary minimum, also measured relative to the primary maximum, is only half as deep on average (0.11 mag). The data from the individual observing runs were folded separately. These four light curves (not shown) are similar to each other and to the master light curve (Fig. 1a). Some of the BV data (not folded) are presented elsewhere (§ IVc; Paper I).

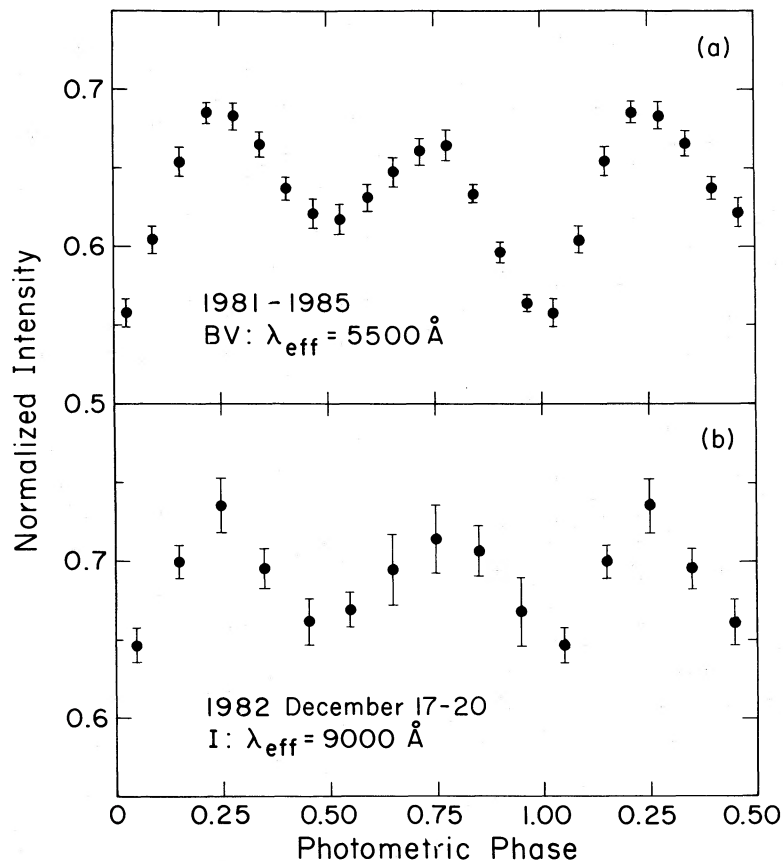


FIG. 1.—(a) The folded light curve at blue-visual wavelengths. Each data point is the mean of ~ 20 -25 separate measurements; the error bars show the rms fluctuations about the mean, and they include both the effects of source fluctuations and counting statistics. The intensity is measured relative to one of the nearby comparison stars: (b) Same as (a) except I-band data with only about four measurements per phase interval.

In Figure 1*b*, the eight hours of I-band data obtained in 1983 are shown folded modulo the orbital period. Despite the poor statistical quality of these data, it is apparent that the I light curve (Fig. 1*b*) and the BV light curve (Fig. 1*a*) are very similar: the I-band data are modulated (≈ 0.14 mag peak-to-peak) at twice the orbital period, and the deeper minimum occurs at photometric phase zero.

c) Ellipsoidal Variations

The tidal forces acting on the K dwarf cause it to deviate from a spherical shape and to have a nonuniform surface brightness. Changes in its geometrical aspect with orbital phase, as seen by a fixed observer, give rise to what are called ellipsoidal light variations.

As we suggested in Paper I, the BV-band light curve (Fig. 1*a*) is primarily due to this ellipsoidal effect—there are two maxima and two minima per orbital cycle. In this passband, however, the accretion disk contributes about half of the total light (see § IV*d*), and it will therefore have a significant influence on the light curve. For example, the unequal maxima in Figure 1*a* are not predicted by the standard ellipsoidal model and may be due to an azimuthal asymmetry in the disk. In the I band the K dwarf probably contributes $\sim 80\%$ of the total light (Oke 1977, § IV*d*), and therefore, the double-humped light curve in Figure 1*b* provides strong confirmation that the light variations are due to the tidal distortion of the companion star.

Apart from coefficients which can be derived from a knowledge of the spectral type, there are three parameters which are constrained by the photometric data in Figures 1*a*–1*b*: the orbital inclination angle i , the radial fraction f of the Roche lobe which is filled, and the mass ratio $q = M_x/M_c$. Consider the I data, which are least affected by the light from the accretion disk. Combining an approximate expression for the amplitude of ellipsoidal variations (Russell 1945; Paper I) with the formula for the mean radius of the Roche lobe, $R_L/a = 0.462(1 + M_x/M_c)^{-1/3}$ (e.g., Warner 1976), we find:

$$f^3 = 0.58(1 + q)/(q \sin^2 i).$$

The gravity darkening and limb darkening coefficients have been evaluated for the case of a K5 dwarf (Lucy 1967; Copeland, Jensen, and Jorgensen 1970; Al-Naimiy 1978) and we have made use of the 0.14 mag amplitude of the I-band light curve. If the above constraint is further combined with the relationship between q and i , which is given below in § V, we reach the following conclusion: if the K dwarf fills its Roche lobe completely ($f \approx 1$), then the inclination of the orbit is $\sim 50^\circ$. At the other extreme, if the orbital inclination is nearly 90° , then the Roche lobe is only 80%–85% filled. Intermediate cases are, of course, possible (e.g., $i \approx 60^\circ$ and $f \approx 0.95$). There is a caveat to this conclusion: Russell's simple formula significantly underestimates the amplitude of the ellipsoidal variations (see Bochkarev, Karitskaya, and Shakura 1979), especially if the Roche lobe is filled or nearly filled. If an exact model were to be used, then one would find smaller values for both i and f . We note that an approximate four-term expression for ellipsoidal variations given by Morris (1985) is similarly inadequate for $f \approx 1$. We conclude that our application requires a full analysis based on Roche geometry.

Bochkarev, Karitskaya, and Shakura (1979) have computed and tabulated a number of ellipsoidal models with Roche geometry for a wide range of parameters. Unfortunately, their calculations do not extend to values of the mass ratio q greater than 3.2, whereas the value of q for A0620-00 is greater than 6

and may be as large as 15–20 (§ V). We nevertheless compared the amplitudes predicted by their models to the observed I-band amplitude for $q = 3.2$ and found that the constraints on i and f are very nearly the same as those given above. However, if the appropriate model results were available for large values of q , we would again find smaller values for both i and f than the ones given above. We note that lower bounds on i and f of $\sim 30^\circ$ and 0.75, respectively, are suggested by an uncertain extrapolation of the results of Bochkarev *et al.*

We tentatively conclude that if $f \approx 1$, then $30^\circ \lesssim i \lesssim 50^\circ$, and if $i \approx 90^\circ$, then $0.75 \lesssim f \lesssim 0.85$. In future work, which will be based on higher quality data and appropriate model calculations, it may be possible to determine the values of both i and f independently.

IV. SPECTRA

a) A First-Order Determination of the Radial Velocities

The only line feature which can be clearly identified in the individual spectra of A0620-00 is H_β in emission. Moreover, H_β is practically the only feature which is apparent when all of the data are summed directly because, as shown below, the photospheric lines of the K dwarf companion are severely Doppler-smearred by orbital motion. Consequently, in order to enhance the detectability of the lines, the individual spectra were cross-correlated against the Doppler-shifted spectrum of a K-dwarf comparison star. The cross-correlation coefficients were computed as a function of the Doppler velocity, V , using the formula

$$CC(V) = \sum_{\lambda} F_{A0620}(\lambda) \times F_K[\lambda(1 + V/c)].$$

The terms F_{A0620} and F_K are the fluxes of A0620-00 and the K-comparison star, respectively. The sum over the wavelength, λ , was taken from 4950–5600 Å, and V was varied from -1500 km s $^{-1}$ to $+1500$ km s $^{-1}$. The calculation was repeated four times, using each of the K-comparison stars in turn as a template. Before the cross-correlation functions were computed, the low-frequency structure in the spectra (wavelength scales > 100 Å) was removed by applying a Fourier (FFT) filter.

The most distinctive feature of the cross-correlation profiles is a prominent peak that systematically shifts with time from large negative velocity to large positive velocity. This phenomenon is robust; for example, it can be seen using the unfiltered data, and any of the four comparison stars (K2–K7) can be used as a template. The velocities which correspond to the central location of the moving peak are plotted in Figure 2. A refined analysis of the velocity data is given below in § IV*c*; therein, and elsewhere in this paper, evidence is presented that the velocity curve in Figure 2 is due to the orbital motion of the K dwarf.

b) Spectrum of A0620-00 in the Rest Frame of the K Dwarf

The sine-wave fit to the velocity data (Fig. 2) was used to Doppler-correct the individual spectra to the approximate rest frame of the K-dwarf secondary. The 10 velocity-shifted spectra were summed and the resultant spectrum was corrected for interstellar reddening $E(B-V) = 0.39$ (Wu *et al.* 1976; Seaton 1979). This grand-sum spectrum and the spectra of the comparison stars are presented in Figure 3.

One hallmark of K dwarfs is clearly present in the summed spectrum of A0620-00: the ~ 200 Å wide depression in the continuum which is due to a combination of MgH ($\lambda 5180$) and the TiO band at $\lambda\lambda 5200$ –4954. This feature has been observed

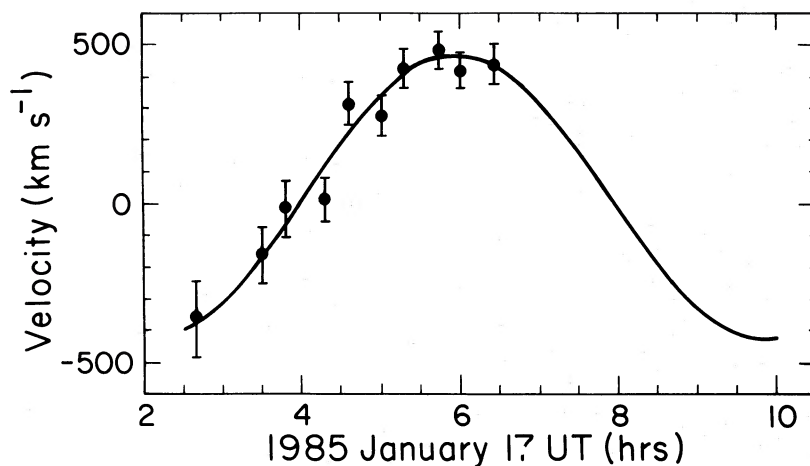


FIG. 2.—A first determination of the radial velocities of the K-dwarf companion obtained by cross-correlating the individual A0620-00 spectra with the spectrum of the K4 V comparison star HR 5568 ($4950 \text{ \AA} \leq \lambda \leq 5600 \text{ \AA}$). A sine-wave fit with the period fixed at the photometric value is shown; the velocity semiamplitude, K , is $444 \pm 60 \text{ km s}^{-1}$.

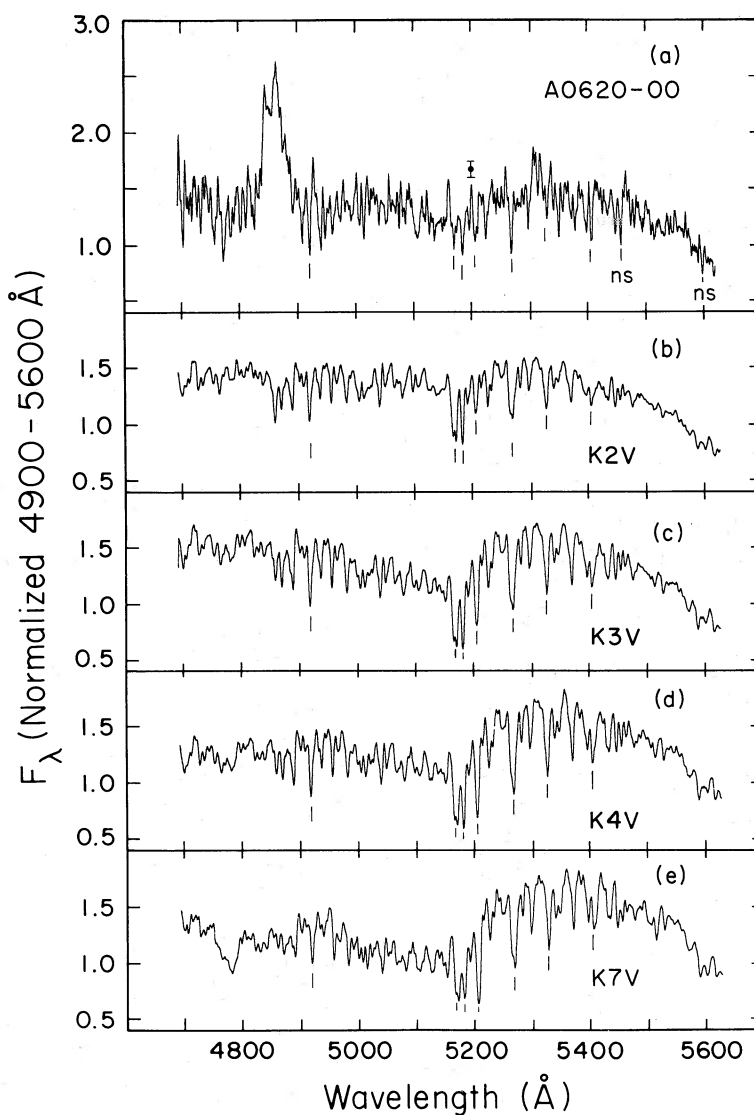


FIG. 3.—Spectra of A0620-00 and four comparison stars plotted in the same rest frame and normalized to have the same average flux longward of H_β . Several photospheric absorption features which are prominent in the comparison spectra are also present in the spectrum of A0620-00: (a) H_β emission dominates the dereddened, summed spectrum of A0620-00. Error bar near 5200 \AA indicates the typical statistical uncertainty ($4900\text{--}5500 \text{ \AA}$) in a 4 \AA band. Uncertainty shortward of H_β is typically 2-3 times larger. Features marked "ns" are artifacts due to emission lines in the night sky; (b)-(e) The continua of the comparison spectra have been corrected for the wavelength-dependent transmission of a neutral density filter. The spectral classifications are from Kennedy and Buscombe (1974) and Buscombe (1981) and references therein.

and discussed previously in studies of A0620-00 (e.g., Oke 1977). The Doppler-corrected spectrum of A0620-00 in Figure 3 also contains a number of photospheric absorption lines or blends which are characteristic of mid-K dwarfs. As expected, these features are not present if all of our data are summed, and Doppler corrections are not applied because the velocity of the secondary varied by 850 km s^{-1} during the course of our observations. This large velocity change corresponds to a wavelength shift of 16 \AA , or 4 times the instrumental resolution. We note also that these features are not evident in previously published spectra of A0620-00 (Oke 1977; Murdin *et al.* 1980). The presence of late-type absorption lines in the Doppler-corrected spectrum of A0620-00 (Fig. 3a) is in itself compelling evidence that we have measured the orbital velocities of the K dwarf.

There are major differences between the spectrum of A0620-00 and the comparison spectra. The presence of an accretion disk in A0620-00, which contributes about half of the continuum flux at 5500 \AA (Oke 1977, § IVd), is responsible for two notable differences: the faintness of the absorption lines and the intense $H\beta$ emission feature (see Oke, § IVe). In addition, the shape of the A0620-00 continuum is altered by the continuum spectrum of the accretion disk (Oke 1977, § IVd).

c) Refined Determination of the Radial Velocities

The cross-correlation analysis described in § IIIa was repeated using the summed spectrum of A0620-00 shown in Figure 3a as a template. The results, which are shown in Figure 4, are very nearly the same as those obtained using one of the comparison stars as a template. As before, there is a well-defined peak which moves smoothly in time. Because the peak has an asymmetric shape, only its central core ($\pm 75 \text{ km s}^{-1}$) was used to locate its center. The velocities were defined to be the values which bisect the area of the central core of the peak. The velocity data, which are listed in Table 2 and plotted in Figure 5a, are well fitted by a simple sinusoid. A comparison of Figure 2 and Figure 5a shows that the residuals are reduced significantly when the summed spectrum of A0620-00 is used as a cross-correlation template.

Values of the orbital parameters and the mass function for a circular orbit are given in Table 3. In the least-squares analysis, the orbital period was fixed at the photometric period, and the velocity data were weighted by their statistical significance. The standard deviations of the velocity data were scaled by a single factor which was adjusted to achieve a χ^2 of 1 per degree of freedom; the 1σ uncertainties in the orbital parameters (Table 3) are based on this prescription.

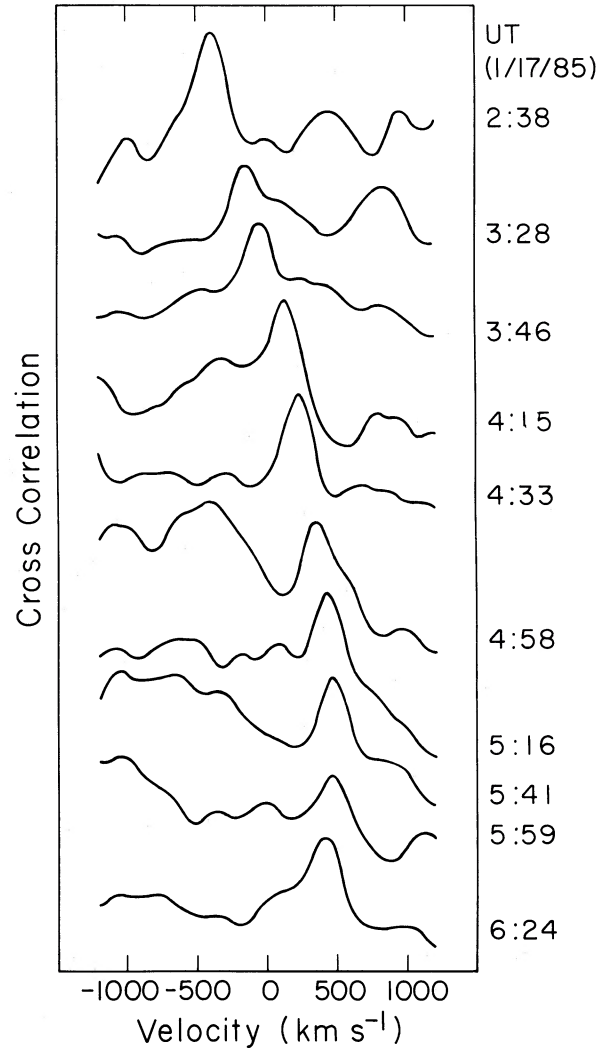


FIG. 4.—Results of a cross-correlation analysis performed on the individual A0620-00 spectra using the summed, rest-frame spectrum (Fig. 3a) as a template. Data with rest-frame wavelengths from $4950\text{--}5600 \text{ \AA}$ were included. A high-pass Fourier filter was first applied to the data (see § IVa).

A comparison between the velocity data (Fig. 5a) and the photometric data (see Fig. 5b) confirms that the velocities are due to the orbital motion of the dwarf companion: the precise photometric period allows for an excellent fit to the radial

TABLE 2
HELIOCENTRIC ABSORPTION-LINE RADIAL VELOCITIES AND
EQUIVALENT WIDTHS OF $H\beta$ IN A0620-00

HJD 2,444,900+	Spectroscopic Phase	Radial Velocities (km s^{-1})	Equivalent Widths of $H\beta$
1182.6143.....	0.586	-383 ± 16	29.2 ± 2.8
1182.6492.....	0.694	-123 ± 12	49.3 ± 3.4
1182.6616.....	0.733	-42 ± 12	30.7 ± 2.1
1182.6819.....	0.795	138 ± 8	48.4 ± 2.3
1182.6945.....	0.834	238 ± 8	34.2 ± 1.6
1182.7118.....	0.888	358 ± 8	29.3 ± 1.4
1182.7243.....	0.926	428 ± 8	49.5 ± 2.4
1182.7419.....	0.981	477 ± 7	20.7 ± 0.9
1182.7543.....	1.019	466 ± 7	24.2 ± 1.0
1182.7716.....	1.073	419 ± 8	28.3 ± 1.3

TABLE 3
ORBITAL PARAMETERS FOR A0620-00^a

Parameter	Circular Orbit Solution
V_0 (km s^{-1})	-5 ± 12
K (km s^{-1})	457 ± 8
T_0^b (spectroscopic)	JD 2,446,082.7481 \pm 0 ^d 0008
T_0^c (photometric)	JD 2,445,477.827 \pm 0 ^d 005
P_{phot} (days)	0.323014 \pm 0.000004
$a_c \sin(i)$ (R_\odot)	2.91 \pm 0.05
$f(M)$ (M_\odot)	3.18 \pm 0.16

^a All quoted uncertainties are 1σ confidence limits.

^b Heliocentric time of maximum velocity.

^c Heliocentric time of primary minimum, agrees with the time of zero velocity to within 5 ± 7 minutes.

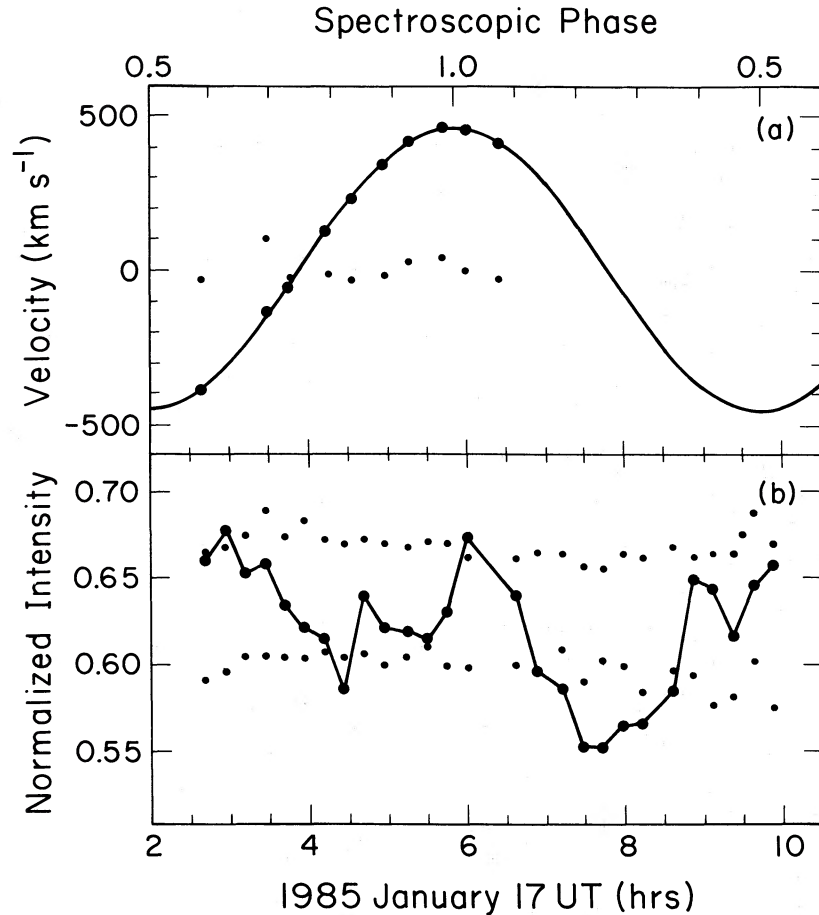


FIG. 5.—(a) Radial velocities of the K dwarf (large filled dots) derived from the cross-correlation analysis described in the text and shown in Fig. 4. Smooth curve is a fit to a circular orbit using the photometric period. Small filled dots are the residual differences ($\times 5$) between the data and the fitted curves; (b) BV-band light curve which was obtained simultaneously with the radial velocity data. Measurement uncertainties ($\sim 2\%$ rms) can be estimated from the light curves of two comparison stars (small dots) which bracket the brightness range of A0620–00.

velocity data; moreover, the time of zero velocity coincides with the time of photometric minimum to within the uncertainties, $\Delta T = 5 \pm 7$ minutes (see Table 3).

d) Component Spectra: Accretion Disk and K Dwarf

Ten months after the 1975 May outburst, Oke (1977) made a detailed study of the spectrum of A0620–00. His findings should be generally applicable to the quiescent state because

the object had faded to its preoutburst brightness, and also because its brightness has subsequently remained fairly constant during the past decade (Table 4). By subtracting the spectrum of a K5 V star from the spectrum of A0620–00, he found a residual spectrum which can be modeled as a power law. Because his observations spanned a broad spectral range, 3200–10000 Å, he was able to obtain quite specific results: he found a power-law index of $\alpha \approx 2.0$ ($F_\lambda \propto \lambda^{-\alpha}$; Oke 1977) and

TABLE 4
VISUAL MAGNITUDE AND EQUIVALENT WIDTH OF H β SINCE OUTBURST

UT Date	V^a	Equivalent Width of H β (Å)	References
1976 May 5	17.6	7.3	Whelan <i>et al.</i> 1977
1976 Oct 3	18.25 ± 0.035	9	Murdin <i>et al.</i> 1980
1976 Nov 16–18	18.35	...	Oke 1977
1976 Dec 17–19	13	Oke 1977; estimated from Fig. 1
1978 Jan 9	18.2 ± 0.1	28	Murdin <i>et al.</i> 1980
1978 Mar 1	25	Murdin <i>et al.</i> 1980
1981 Oct 29–Nov 3	17.8–18.1	...	Paper I; this paper
1982 Dec 15–20	17.9–18.2	...	This paper
1983 Dec 6–16	17.8–18.1	...	This paper
1985 Jan 12–17	17.7–18.0	33	This paper

^a At present there is an uncertainty in the zero point of the 1981–1985 V-band data of ~ 0.3 mag.

a fraction of the total V-band light due to the disk of $f_{5500} = 0.43 \pm 0.06$.

We also have attempted to achieve a decomposition of the spectrum into a power-law component, which we ascribe to the accretion disk, plus a component due to a K dwarf. We generated model spectra by adding power-law components to the K comparison spectra (Fig. 3b-3e). The model spectra were normalized to have the same flux (4900-5600 Å) as the spectrum of A0620-00 (Fig. 3a). The parameters which characterize the disk spectrum (α and f_{5500}) were varied, and a χ^2 comparison was made between the spectrum of A0620-00 and each of the comparison spectra in turn. None of the models provided a good fit to the spectrum of A0620-00; moreover, because of the limited spectral coverage, the χ^2 minima are very broad. Nevertheless, our results tend to support Oke's findings: for a K4 V star (Fig. 3d) plus a disk, we find that the best match is achieved for $\alpha = 2.5 \pm 1.0$ and $f_{5500} = 0.4 \pm 0.1$. Although the derived power-law index is very sensitive to the spectral type of the model, the fraction of the light contributed by the disk is not: in passing from K3 to K7 the value of f_{5500} increases only slightly from 0.35 to 0.47.

We conclude that the continuum spectrum of the accretion disk contributes slightly less than half of the total V-band light and can be approximately represented by a power law, $F_\lambda \propto \lambda^{-2.0}$. A smooth disk spectrum of this form was subtracted from the observed spectrum of A0620-00 to reveal the residual spectrum of the K star. The result, shown in Figure 6a, is plotted with the same normalization of the continuum as Figures 6b-6g. Interestingly, the lines in the residual spectrum (Fig. 6a) appear to be somewhat narrower and deeper than the corresponding lines in the comparison stars. Nearly all of the prominent features in the comparison spectra (Figs. 6c-6f) are apparent in the Doppler-corrected spectrum of A0620-00 (Figs. 6a and 6b), whereas none of these features appear convincingly in the direct-sum (i.e., no Doppler correction) spectrum shown in Figure 6g.

e) Balmer Emission

The accretion disk is thought to be responsible for the broad H_β emission feature which dominates the spectrum of A0620-00 (Fig. 3a; see § I and references therein). In a direct sum of all of our data (i.e., no Doppler corrections applied), the full width of the feature is 2200 km s^{-1} at half-maximum intensity and 4460 km s^{-1} at zero intensity, which is about the same as the value reported previously by Murdin *et al.* (1980). If the width of the line is due to disk rotation, it implies that the highest-velocity Balmer emission must originate fairly close to the compact object (Keplerian radius $\sim 0.2 R_\odot$ for the models discussed below).

An examination of the 10 individual spectra revealed gross variations in the shape and intensity of the feature. A few of the short-exposure H_β profiles are as broad as the summed profile, while others are about half as wide. In some cases, the center of a profile is shifted redward or blueward from the center of the summed profile; however, no systematic orbital variations are apparent. A good measure of the erratic variability of the H_β feature is given by its equivalent width, which was observed to vary by more than a factor of 2 in 30 minutes (Table 2). We conclude that it may prove impossible to detect the orbital motion of the compact object because its velocity will not be large ($K_x \lesssim 70 \text{ km s}^{-1}$) and because the H_β line is very broad and erratically variable.

V. THE MASS OF THE COMPACT SOURCE

a) The Mass Function

An absolute 3σ lower limit to the mass of the compact X-ray source (M_x) of $2.70 M_\odot$ is given by the value of the mass function itself, $f(M) = (M_x \sin i)^3 / (M_x + M_c)^2 = 3.18 \pm 0.16$ (Table 3), where M_c is the mass of the companion. This limiting value of M_x corresponds to a companion star with zero mass; this is illustrated in Figure 7a, which is a plot of M_x versus M_c for three values of the orbital inclination angle. It is evident that the value of M_x is only weakly dependent on the mass of the companion. A range of K-star masses that corresponds to a liberal estimate of the uncertainties in the spectral type, K2-K7, (see Oke 1977; Murdin *et al.* 1980) is indicated in Figure 7a.

The small dependence of M_x on M_c is also apparent in Figure 7b, which is a plot of M_x versus inclination angle. As indicated in the lower right corner of Figure 7b, a weak constraint can be placed on M_x because no X-ray eclipses were observed during the 1975 outburst. The constraint, as shown, is based on a zero-age main-sequence (ZAMS) mass-radius relationship, although it does not matter very much what mass-radius relationship is assumed (e.g., see Copeland, Jensen, and Jorgensen 1970).

A firm lower limit on the mass of the compact object can be obtained as follows. If the companion star is on the zero-age main sequence, then its mid-K spectral type implies that its mass is between $\sim 0.5 M_\odot$ and $0.8 M_\odot$ (Fig. 7). Because some X-ray binaries are known to be undermassive for their spectral type (e.g., see Cowley and Crampton 1975; Mason *et al.* 1982), we make the conservative assumption that the mass of the companion is only $0.25 M_\odot$, which is the measured mass of the \sim K2 IV secondary in the old nova GK Per (Watson, King, and Osborne 1985). For $M_c = 0.25 M_\odot$, $i = 85^\circ$ (absence of X-ray eclipses), and a K velocity which is 3σ less than the best-fit value (Table 3), we find $M_x = 3.20 M_\odot$. Therefore, a firm 3σ lower limit to the mass of the compact object is $3.20 M_\odot$. This limit exceeds the maximum allowed mass of a stable neutron star for a broad range of possible equations of state considered by Arnett and Bowers (1977)—the most realistic and sophisticated models of nonrotating neutron stars imply a maximum mass of $2.0 M_\odot$, and even the stiffest equation of state predicts a maximum mass of only $2.7 M_\odot$. Moreover, calculations indicate that rotation cannot increase the maximum mass by more than $\sim 20\%$ (see Shapiro and Teukolsky 1983, p. 264, and references therein). The above limit also exceeds the maximum neutron-star mass of $\sim 3 M_\odot$ which is allowed by general relativity and causality (Rhoades and Ruffini 1974; Chitre and Hartle 1976). In this sense, we conclude that the compact object in A0620-00 is a black hole.

A more realistic lower bound on M_x can be set by using the preferred spectral type and mass of the companion (K5 V and $0.7 M_\odot$) and the absence of X-ray eclipses ($i \lesssim 80^\circ$). In this case we find $M_x > 4.0 M_\odot$ (3σ). In addition, if the companion fills its Roche lobe and we invoke the constraint on the inclination angle imposed by the amplitude of the ellipsoidal variations ($i < 50^\circ$; § IIIc), we find $M_x > 7.3 M_\odot$ (3σ).

b) Systematic Errors

There are four effects that may modify the velocity amplitude and reduce the limiting value of M_x : X-ray heating, tidal distortion, nonsynchronous rotation, and spectral contamination by emission lines. These effects may displace the photo-

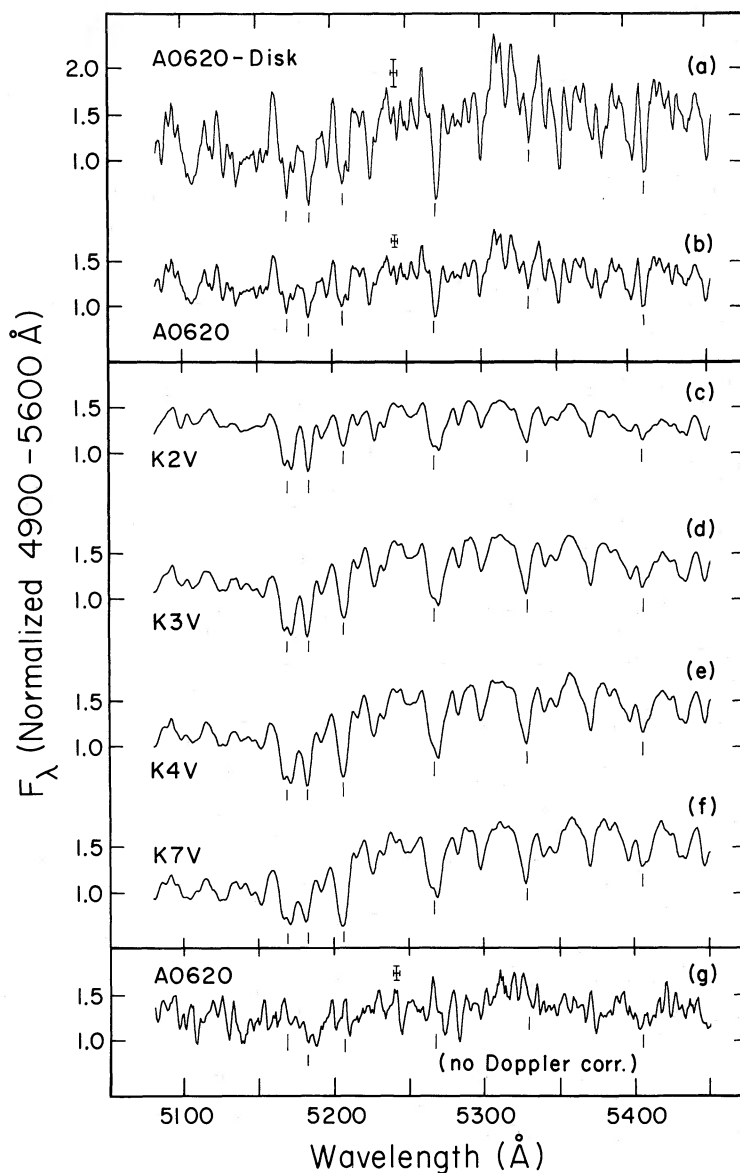


FIG. 6.—A blowup of the central portion of the spectra shown in Fig. 3. Vertical error bars are the statistical uncertainties in a 4 \AA band (indicated by horizontal bars) which corresponds to the instrumental resolution. (a) Rest-frame spectrum of A0620-00 with power-law disk component subtracted (see text); (b) A blowup of the rest frame spectrum shown in Figure 3a (no disk component subtracted); (c)–(f) comparison spectra as shown previously in Fig. 3b–3e. Most of the prominent features are blends of lines of neutral Mg, Fe, Cr, and Ti and are significantly broader than the instrumental resolution; (g) Summed spectrum of A0620-00 with no Doppler corrections applied. Note that the photospheric features, which are present in (a) and (b) and in the comparison spectra, are absent in this spectrum.

center of the K dwarf, as measured in the light of the absorption lines, away from its center of mass. In the following we consider the four effects in turn and conclude that they are unlikely to significantly alter the conclusions reached above.

We first consider the heating effect. For some systems (e.g., HZ Her; see Crampton and Hutchings 1972), the masses inferred from radial velocity data are affected significantly by X-ray heating. However, for A0620-00 it is likely that the effects of X-ray heating are negligible for the following reasons. First, the absence of detectable X-radiation from A0620-00 in quiescence ($L_x < 10^{32} \text{ ergs s}^{-1}$) implies that the temperature difference between the heated and unheated hemispheres is negligible ($\lesssim 10 \text{ K}$; see Paper I). Second, one expects the most intense X-ray or ultraviolet heating and the bluest color to occur at spectroscopic phase 0.25 (photometric phase zero),

which is, in fact, the time of the primary minimum in both the BV-band and I-band light curves. Moreover, the color of the system is somewhat redder at spectroscopic phase 0.25 than at other times (see Figs. 1a and 1b). We conclude that the radial velocity measurements are not affected by heating of the optical star.

A second influence on the amplitude of the velocity curve is tidal distortion. The observed ellipsoidal light variations (see § IIIc) reveal that the K dwarf is tidally distorted and has a nonuniform surface brightness. This nonuniformity may cause the centers of the absorption lines to shift toward higher velocity. Using an approximate expression from Sterne (1941), we find that these effects do not contribute more than 0.3% to the observed velocity amplitude. Sterne's formula assumes that the star is an ellipsoid and, consequently, it somewhat underesti-

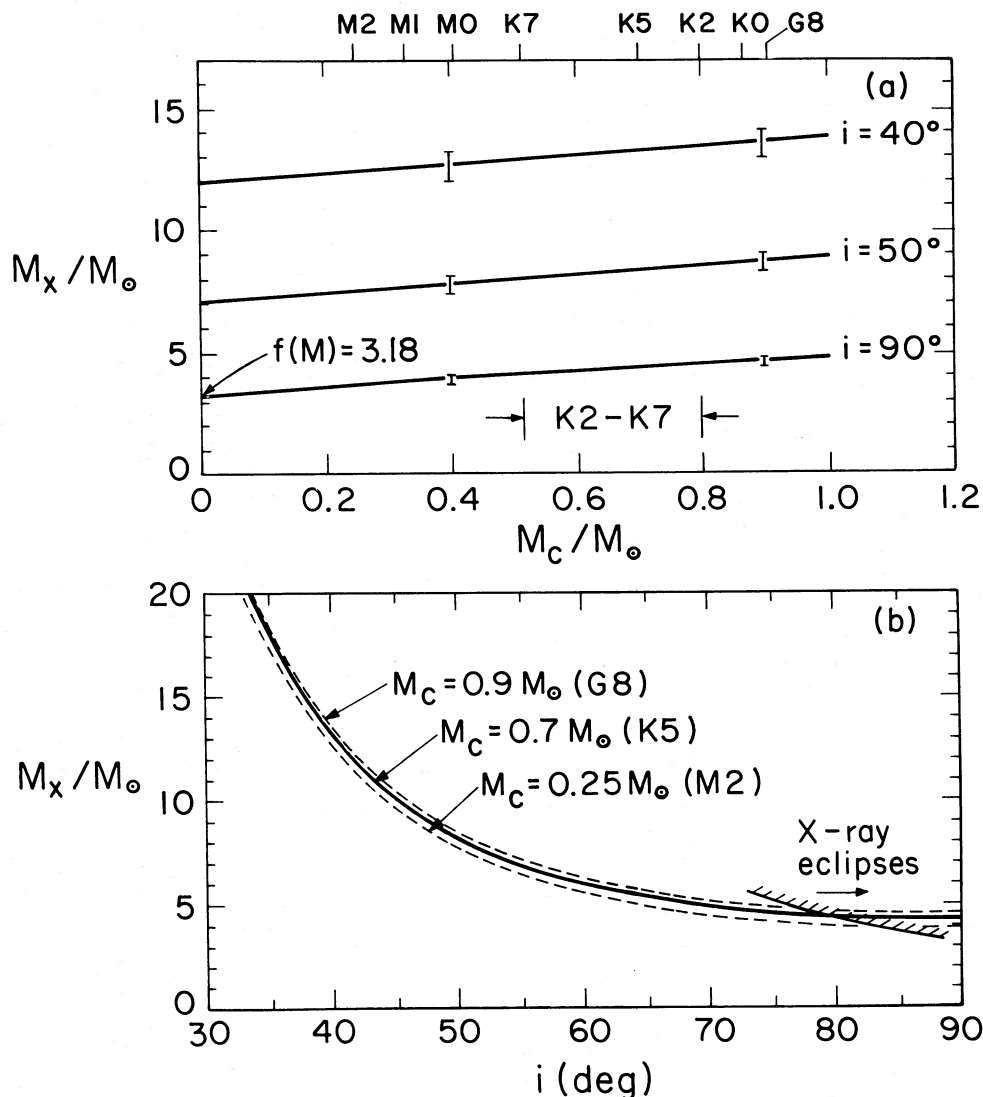


FIG. 7.—(a) Because of the large inverted mass ratio, the mass of the compact object is only weakly dependent on the mass of the companion. As indicated, the spectral type of the companion is unlikely to be later than K7 or earlier than K2. The correspondence between spectral type and mass is for a ZAMS model ($x = 0.700$, $y = 0.270$, and $z = 0.030$) by Copeland, Jensen, and Jorgensen (1970); (b) Mass of the compact source vs. orbital inclination for three values of M_c . As shown, the failure to observe X-ray eclipses rules out very highly inclined orbits.

mates the tidal effects. Nevertheless, it is improbable that the effects of tidal distortion contribute more than $\sim 1\%$ to the velocity amplitude; a firmer conclusion must await an analysis based on Roche-lobe geometry.

A magnification of the effects of heating and tidal distortion could occur if the rotation period of the K dwarf is not phase-locked at the orbital period. It is possible that occasional deviations from synchronous rotation do occur under the influence of mass exchange or the loss of mass and angular momentum from the system. Such deviations, however, are expected to be small and short-lived because the time scale for synchronization is estimated to be $\lesssim 1000$ yr (Zahn 1977, eq. [6.1]). We also note that the absorption lines of A0620-00 are relatively narrow (Figs. 6a and 6b); their widths are consistent with the expected corotational velocity (≈ 110 km s $^{-1}$ for $R_c = 0.7 R_\odot$) and rule against large departures from corotation. It therefore appears unlikely that nonsynchronous rotation will significantly affect the observed velocities.

Finally, in some mass-exchange binaries, systematic errors in the absorption-line velocities are due to blending with emission lines from an accretion disk or circumstellar material (e.g., Moulding 1977). This effect should not be a significant problem in A0620-00. If the accretion disk emits lines of Mg I, Fe I, etc., their velocity amplitudes should reflect the orbital motion of the compact object and therefore be relatively small ($K_x \lesssim 70$ km s $^{-1}$). On the other hand, the orbital motion of the K dwarf modulates the observed wavelengths of the absorption lines with a full amplitude of 16 \AA , which is ~ 10 times their width (for an assumed corotational velocity of the K dwarf of 110 km s $^{-1}$). Consequently, for most of the orbital cycle, an absorption line and its emission-line counterpart will be cleanly separated and the radial velocity data should not be affected by blending. Here we have assumed that the emission lines of the neutral metals come from the cooler, outer portions of the disk and are therefore fairly narrow ($\lesssim 5 \text{ \AA}$). If the emission lines are broad ($\gtrsim 10 \text{ \AA}$), their effects will also be small. A

broad emission line is unlikely to produce significant changes in the shape of the continuum on the scale that corresponds to the widths of the absorption lines ($\lesssim 2 \text{ \AA}$). Finally, no matter whether the putative emission lines are broad or narrow, the center of an absorption line cannot shift by more than a fraction of its width ($\lesssim 2 \text{ \AA}$), which corresponds to a small fraction of the observed Doppler modulation (16 \AA).

VI. DISCUSSION

It is reasonable to expect that the luminous X-ray source is fed by Roche lobe overflow. It is possible that mass transfer occurs only during times of eruption; for example, it might be triggered by an episodic swelling of the dwarf companion. On the other hand, it is also possible that a low level of mass transfer ($\sim 3 \times 10^{-11} M_{\odot} \text{ yr}^{-1}$; Paper I) is occurring continually during quiescence, as suggested by the variability in the Balmer emission (§ IVe). If so, it is unlikely that the accreted gas is flowing continually onto the compact source because no X-rays are detected in quiescence (e.g., $L_x < 10^{32} \text{ ergs s}^{-1}$; Paper I). In this case, it may be that matter is accumulated and stored in the accretion disk for decades until an instability releases it onto the compact object. Such a model has been proposed to account for the outbursts of dwarf novae (e.g., Meyer and Meyer-Hofmeister 1981; Faulkner, Lin, and Pappalozou 1985, and references therein; Canizzo, Wheeler, and Ghosh 1985).

Do we expect the dwarf companion to fill its Roche lobe if it is a normal main-sequence star with a spectral type near K5? Combining Kepler's law with the relationship for the mean Roche lobe radius (see § IIIc), we find that R_L depends only on the mass of the companion: $R_L/R_{\odot} = 0.92(M_c/M_{\odot})^{1/3}$. Comparing this expression to an approximate mass-radius relationship for Population I stars of zero age on the lower main sequence, $R/R_{\odot} = 0.93 M/M_{\odot}$ (Robinson 1976; Copeland, Jensen, and Jorgensen 1970; Popper 1980), we find that a companion with a mass less than the mass of the Sun ($G2$) is not expected to fill its Roche lobe. (For a Population II star an even greater mass is required; e.g., see Copeland *et al.* 1970). Because the preferred spectral type of the companion is $\sim K5$ ($0.7 M_{\odot}$) and because it is almost certainly not earlier than K2 ($0.8 M_{\odot}$), we conclude that either the optical star does not fill its Roche lobe or the radius of the companion significantly exceeds its main-sequence value (see Fig. 8). The latter condition (evolved secondary) has also been inferred for several other X-ray binaries, including Sco X-1 (Cowley and Cramp-ton 1975) and 4U 1822-37 (Mason *et al.* 1982).

Cyg X-1 and LMC X-3 are leading black hole candidates (Gies and Bolton 1986, and references therein; Cowley *et al.* 1983); the evidence is based on firm dynamical measurements.³ A0620-00 is the third black-hole candidate determined from an analysis of the binary orbital parameters. A number of other sources (e.g., GX 339-4 and Cir X-1) have been suggested as black-hole candidates based on nondynamical arguments. In particular, rapid X-ray flickering, which is observed for Cyg X-1, has long been thought to be a bona fide signature of a black hole. Recent observations, however, of rapid flickering in the pulsating, neutron-star binary V0332+53 have undermined this belief (Stella *et al.* 1985). Recently a new signature of a black hole was suggested by White, Kaluzienski, and Swank

³ LMC X-1 may also contain a black hole; however, the dynamical evidence is less compelling. Moreover, the orbital period and the optical identification are somewhat uncertain (Hutchings, Crampton, and Cowley 1983).

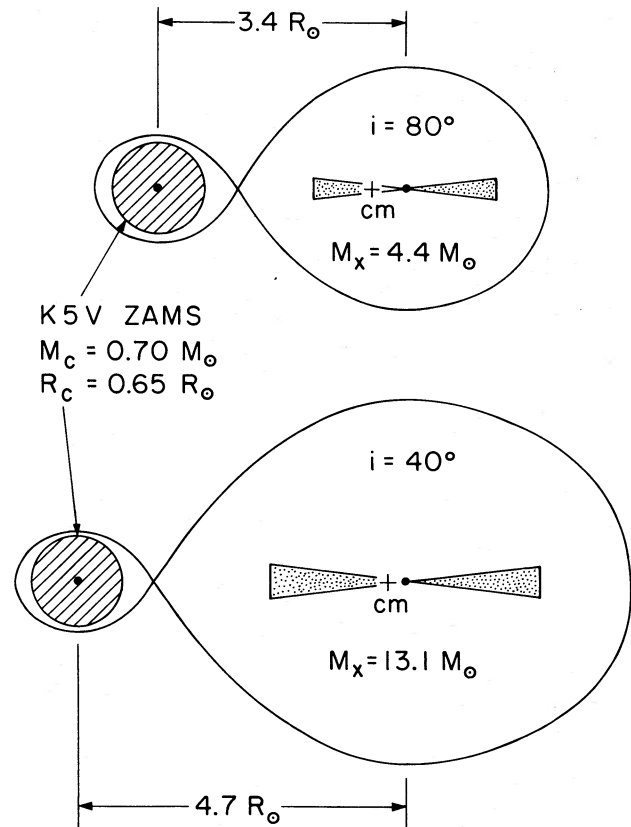


FIG. 8.—Schematic sketch, to scale, of A0620-00 for two values of the orbital inclination and for a K5 V ZAMS companion. The principal dimensions of the Roche lobes were taken from Kopal (1959) and Plavec and Kratochvíl (1964). The view is in the orbital plane and the stippled region centered on the compact object represents an accretion disk whose size is not known. As shown, the K5 main-sequence star fails to fill its Roche lobe (see § VI).

(1984) and White and Marshall (1984), who found that the leading black-hole candidates, including Cyg X-1 (high state) and LMC X-3, have extremely soft X-ray spectra in the range 1–10 keV. They suggested that several X-ray sources with similarly soft X-ray spectra, including A0620-00, should be regarded as potential black-hole candidates. The results presented in this paper provide strong support for their hypothesis. We note that Coe, Engel, and Quenby (1976) were the first to point out the spectral similarity of A0620-00 and Cyg X-1.

A neutron star or a black hole is thought to be formed by the core collapse of a massive ($\gtrsim 5-8 M_{\odot}$) star. It is possible that only the most massive progenitor stars spawn black holes. However, on theoretical grounds alone this conjecture is very uncertain because the final stages of evolution of massive stars are poorly understood (e.g., Arnett 1979). Progress in determining the lower mass limit of black-hole progenitors was made recently by van den Heuvel and Habets (1984). They used the black-hole candidate LMC X-3 and the neutron-star binary 4U 1223-62, plus considerations on the evolutionary histories of these systems, to conclude that a star must be initially at least as massive as $40 M_{\odot}$ to terminate its life as a black hole.

Based on the evolutionary history inferred for LMC X-3 by van den Heuvel and Habets, A0620-00 may initially have been a wide binary composed of an unevolved 40–80 M_{\odot} star and a late-type dwarf with an orbital period of a month or

more. In this scenario the primary star lost $\sim 10\text{--}20 M_{\odot}$ to stellar winds prior to engulfing the secondary. After the common envelope was established, mass was transferred to the dwarf companion and the stars spiraled toward each other. The common envelope was ejected from the system on a short time scale because of frictional heating. After the spiral-in, the orbital period was a fraction of a day and the massive star had been reduced to a $\sim 20\text{--}30 M_{\odot}$ helium core. During its lifetime the core shed several more solar masses of material via a stellar wind before it detonated to form the $\sim 10 M_{\odot}$ black hole. Strong tidal forces rapidly circularized the orbit following the supernova explosion.

If this scenario is applicable to A0620-00, then remarkably little of the envelope (or wind-driven gas) was accreted by the dwarf companion; its present mass is only $\sim 0.7 M_{\odot}$. Furthermore, if we assume that the companion has been losing mass to the black hole at the current average rate ($\sim 3 \times 10^{-11} M_{\odot} \text{ yr}^{-1}$; see Paper I) for a Hubble time, its initial mass was only $\sim 1.3 M_{\odot}$. A possible problem with this scenario, an apparent lack of suitable progenitor systems, was pointed out to us by P. Conti. There is circumstantial evidence that low-mass secondaries are not present in O-star binaries (Garmany, Conti, and Massey 1980).

As an alternative, it is possible that the initial mass of the companion was much larger, perhaps several or more solar masses, and that its rate of mass loss was also much larger in the past. In this case, perhaps the supernova explosion of the primary first formed a neutron star which was subsequently pushed over the neutron-star mass limit by the gradual accretion of gas. If the initial mass of the neutron star was $\sim 1.4 M_{\odot}$ (e.g., Arnett 1979; Joss and Rappaport 1984), then at least $1.8 M_{\odot}$ of material must have been stripped from the companion to produce the compact object we now observe (§ V). If so, good-quality spectra obtained in future observations may reveal that the companion is the core of a more massive progenitor. We note that the presence of intense H_{β} emission (§ IVe) indicates that the secondary contains an appreciable amount of hydrogen and it is therefore not a pure helium core.

An 8.2 hr X-ray period has been suggested for Cen X-4

(Kaluziński, Holt, and Swank 1980), another X-ray nova which is very similar in its optical properties to A0620-00 (see Figs. 5d and 5e in Bradt and McClintock 1983, and references therein). Its compact X-ray source, however, is almost certainly a neutron star; it has been observed to emit Type I X-ray bursts (Matsuoka *et al.* 1980). It should be possible to determine the mass of the compact source in Cen X-4 by measuring the radial velocity and ellipsoidal variations of its K-dwarf companion. A comparative study of A0620-00 and Cen X-4 may prove to be a fruitful way to examine the differences and similarities between black-hole binaries and neutron-star binaries.

We are especially grateful to W. A. Hiltner, founder of the McGraw-Hill Observatory, and to M. Johns, the on-site director, and to several other people for ample access to the excellent facilities of the McGraw-Hill Observatory. We are also grateful to G. Ricker and his colleagues for making the MASCOT CCD camera available to us and to W. H. G. Lewin for his help in carrying out the 1983 CCD observations under difficult circumstances. Much of the CCD data were skillfully analyzed by two MIT undergraduates, M. Scott and C. Covault. We thank several KPNO staff members for their generous support of our 4 m observations: in particular, J. DeVeny and J. Barnes, and also C. Mahaffey, who brought the IIDS back into operation in the eleventh hour. L. Petro, who helped initiate this study in 1981 (Paper I), has continued to provide valuable counsel. We are also indebted to G. W. Clark for his long-term support of our work, to Y. Avni and S. Rappaport for helpful discussions, and to several other people, including A. Cowley and D. Lamb, for their comments on a draft of the manuscript. The principal financial support for this work was provided by the National Science Foundation under grants AST 81-15557 and AST 84-14597. Additional support was provided by the National Aeronautics and Space Administration under grant NSG7643. J. E. McClintock gratefully acknowledges the support of the Smithsonian Institution during the preparation of this manuscript.

REFERENCES

- Al-Naimiy, H. M. 1978, *Ap. Space Sci.*, **53**, 181.
 Arnett, W. D. 1979, in *Sources of Gravitational Radiation*, ed. L. Smarr (Cambridge: Cambridge University Press), p. 311.
 Arnett, W. D., and Bowers, R. L. 1977, *Ap. J. Suppl.*, **33**, 415.
 Barnes, J., *et al.* 1983, *IPPS-IIDS/IRS Reduction Manual* (Tucson: KPNO).
 Bochkarev, N. G., Karitskaya, E. A., and Shakura, N. I. 1979, *Soviet Astr.*, **23**, 8.
 Boley, F., Wolfson, R., Bradt, H., Doxsey, R., Jernigan, G., and Hiltner, W. A. 1976, *Ap. J. (Letters)*, **203**, L13.
 Bradt, H. V. D., and McClintock, J. E. 1983, *Ann. Rev. Astr. Ap.*, **21**, 13.
 Buscombe, W. 1981, *Fifth General Catalogue of MK Spectral Classifications* (Evanston: Northwestern University Press).
 Canizzo, J. K., Wheeler, J. C., and Ghosh, P. 1985, in *Cataclysmic Variables and Low-Mass X-ray Binaries*, ed. D. Q. Lamb and J. Patterson (Dordrecht: Reidel), p. 307.
 Chitre, D. M., and Hartle, J. B. 1976, *Ap. J.*, **207**, 592.
 Coe, M. J., Engel, A. R., and Quenby, J. J. 1976, *Nature*, **259**, 544.
 Copeland, H., Jensen, J. O., and Jorgensen, H. E. 1970, *Astr. Ap.*, **5**, 12.
 Cowley, A. P., and Crampton, D. 1975, *Ap. J. (Letters)*, **201**, L65.
 Cowley, A. P., Crampton, D., Hutchings, J. B., Remillard, R., and Penfold, J. E. 1983, *Ap. J.*, **272**, 118.
 Crampton, D., and Hutchings, J. B. 1972, *Ap. J. (Letters)*, **178**, L65.
 DeVeny, J. 1984, *An Observer's Manual for the Intensified Image Dissector Scanner* (Tucson: KPNO).
 Elvis, M., Page, C. G., Pounds, K. A., Ricketts, M., and Turner, M. J. L. 1975, *Nature*, **257**, 656.
 Faulkner, J., Lin, D. N. C., and Papaloizou 1985, in *Cataclysmic Variables and Low-Mass X-ray Binaries*, ed. D. Q. Lamb, and J. Patterson (Dordrecht: Reidel), p. 315.
 Garmany, C. D., Conti, P. S., and Massey, P. 1980, *Ap. J.*, **242**, 1063.
 Gies, D. R., and Bolton, C. T. 1986, *Ap. J.*, **304**, 391.
 Goad, L. 1985, private communication.
 Hutchings, J. B., Crampton, D., and Cowley, A. P. 1983, *Ap. J. (Letters)*, **275**, L43.
 Joss, P. C., and Rappaport, S. 1984, *Ann. Rev. Astr. Ap.*, **22**, 537.
 Kaluziński, L. J., Holt, S. S., and Swank, J. 1980, *Ap. J.*, **241**, 779.
 Kennedy, P. M., and Buscombe, W. 1974, *MK Spectral Classifications* (Evanston: Northwestern University).
 Kopal, Z. 1959, *Close Binary Systems* (New York: Wiley).
 Lucy, L. B. 1967, *Zs. Ap.*, **65**, 89.
 Mason, K. O., Murdin, P. G., Tuohy, I. R., Seitzer, P., and Branduardi-Raymont, G. 1982, *M.N.R.A.S.*, **200**, 793.
 Matsuoka, M., *et al.* 1980, *Ap. J. (Letters)*, **240**, L137.
 McClintock, J. E., Petro, L. D., Remillard, R. A., and Ricker, G. R. 1983, *Ap. J. (Letters)*, **266**, L27 (Paper I).
 Meyer, F. and Meyer-Hofmeister, E. 1981, *Astr. Ap. (Letters)*, **104**, L10.
 Morris, S. L. 1985, *Ap. J.*, **295**, 143.
 Moulding, M. 1977, *Astr. Ap.*, **58**, 393.
 Murdin, P., Allen, D. A., Morton, D. C., Whelan, J. A. J., and Thomas, R. M. 1980, *M.N.R.A.S.*, **192**, 709.
 Oke, J. B. 1977, *Ap. J.*, **217**, 181.
 Plavec, M. and Kratochvil, P. 1984, *Bull. Astr. Inst. Czechoslovakia*, **15**, No. 5, 165.
 Popper, D. M. 1980, *Ann. Rev. Astr. Ap.*, **18**, 115.
 Rhoades, C. E., and Ruffini, R. 1974, *Phys. Rev. Letters*, **32**, 324.
 Ricker, G. R., Bautz, M. W., Dewey, D., and Meyer, S. S. 1981, *Proc. Soc. Photo-Opt. Instrum. Eng.*, **290**, 190.
 Robinson, E. L. 1976, *Ann. Rev. Astr. Ap.*, **14**, 119.

- Russell, H. N. 1945, *Ap. J.*, **102**, 1.
 Seaton, M. J. 1979, *M.N.R.A.S.*, **187**, 73P.
 Shapiro, S. L., and Teukolsky, S. A. 1983, *Black Holes, White Dwarfs, and Neutron Stars* (New York: Wiley).
 Stella, L., White, N. E., Davelaar, J., Parmar, A. N., Blissett, R. J., and van der Klis, M. 1985, *Ap. J. (Letters)*, **288**, L45.
 Sterne, T. E. 1941, *Proc. Nat. Acad. Sci.*, **27**, 168.
 van den Heuvel, E. P. J., and Habets, G. M. H. J. 1984, *Nature*, **309**, 598.
 van Paradijs, J. 1983, in *Accretion Driven Stellar X-ray Sources*, ed. W. H. G. Lewin and E. P. J. van den Heuvel (Cambridge: Cambridge University Press) p. 189.
 Warner, B. 1976, in *Structure and Evolution of Close Binary Systems*, ed. P. Eggleton, S. Mitton, and J. Whelan (Dordrecht: Reidel), p. 85.
 Watson, M. G., King, A. R., and Osborne, J. 1985, *M.N.R.A.S.*, **212**, 917.
 Whelan, J., et al. 1977, *M.N.R.A.S.*, **180**, 657.
 White, N. E., Kaluzienski, J. L., and Swank, J. H. 1984, in *High Energy Transients in Astrophysics*, ed. S. E. Woosley (New York: AIP), p. 31.
 White, N. E., and Marshall, F. E. 1984, *Ap. J.*, **281**, 354.
 Wu, C.-C., Aalders, J. W. G., van Duinen, R. J., Kester, D., and Wesselius, P. R. 1976, *Astr. Ap.*, **50**, 445.
 Zahn, J.-P. 1977, *Astr. Ap.*, **57**, 383.

Note added in proof.—A preliminary analysis of spectroscopic data that we obtained with the Multi Mirror Telescope on 1985 December 11 confirms the result presented in this paper.

JEFFREY E. McCLINTOCK: Harvard-Smithsonian Center for Astrophysics, 60 Garden Street, Cambridge, MA 02138

RONALD A. REMILLARD: Massachusetts Institute of Technology, Center for Space Research, Room 37-495, Cambridge, MA 02139